Available online at www.HEFJournal.org

ISSN: 2785-2997

Journal of
Human, Earth, and Future

Vol. 7, No. 2, June, 2026

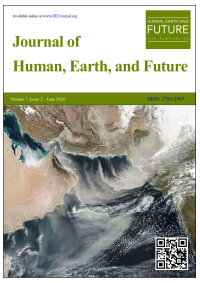

Influence of In Situ Stress on Rockburst Potential and Deformation Behavior in Deep Rock Masses

A. Imashev [1], G. Yeskenova [1*], Melih Geniş [2], A. Suimbayeva [1], G. Zhunusbekova [1]

[1] *Abylkas Saginov Karaganda Technical University, Karaganda, 100012, Kazakhstan.*

[2] *Department of Mining Engineering, Zonguldak Bülent Ecevit University, Zonguldak 67100, Türkiye.*

Received 26 March 2026; Revised 17 May 2026; Accepted 20 May 2026; Published 01 June 2026

Abstract

As underground mining operations advance to greater depths, increasingly complex geomechanical conditions require reliable assessment of the stress–strain state of the surrounding rock mass to ensure excavation stability and safety. The objective of this study is to investigate the influence of in-situ stress conditions on stress redistribution, yielded zone development, and rockburst susceptibility around deep underground excavations. Numerical modeling was performed using the finite element method implemented in Rocscience RS2 for mining depths ranging from 600 to 1500 m and different lateral stress coefficients. The Hoek–Brown failure criterion was adopted to evaluate rock mass stability and identify yielded zones, while rockburst susceptibility was assessed using the Turchaninov, Wang, and Castro criteria. The results demonstrate that increasing mining depth significantly increases stress concentration around excavations and promotes the expansion of yielded zones. The spatial distribution of deformation and yielded zones is strongly controlled by stress anisotropy, represented by the ratio between horizontal and vertical stresses. Higher lateral stress coefficients redistribute deformation from the roof and floor toward the sidewalls, altering the dominant failure mechanisms. All applied criteria indicate a systematic increase in rockburst susceptibility with depth, although the predicted hazard levels differ among the methods. The novelty of this study lies in the integrated assessment of stress concentration, deformation localization, yielded zone evolution, and rockburst susceptibility within a unified numerical framework. The findings contribute to improved stability assessment, support design, and geotechnical risk management in deep underground mining.

Keywords: In-Situ Stress; Deep Mining; Numerical Modeling; Finite Element Method; Geological Strength Index (GSI); Yielded Zones; Lateral Pressure Coefficient; Excavation Stability; Rockburst Susceptibility.

1. Introduction

The long-term exploitation of mineral resources in Kazakhstan has resulted in a substantial depletion of reserves at shallow and intermediate depths, thereby driving a sustained transition toward deep-level mining. In major mining regions, including both metal and coal mining districts, underground operations have reached depths of 500–600 m, while in several deposits mining activities extend beyond 800–1000 m. This shift toward deep mining is accompanied by significant transformations in geomechanical conditions, including increased rock pressure, an enhanced contribution of horizontal tectonic stresses, and more complex interactions between the rock mass and underground excavations. Under these circumstances, there is an increasing demand for advanced geomechanical analysis techniques, particularly those based on numerical modeling of the stress–strain state and the accurate characterization of the initial stress field for the design and stability assessment of underground structures.

* Corresponding author: g.eskenova@ktu.edu.kz

https://doi.org/10.28991/HEF-2026-07-02-016

Within this framework, the in-situ stress state is recognized as a governing factor controlling the mechanical behavior of the rock mass during underground mining. The geostatic stress field constitutes the primary loading condition, defining the initial deformation state and regulating the redistribution of stresses induced by excavation processes [1, 2]. It exerts a direct influence on excavation stability, the selection of support systems, and the mechanisms of rock mass failure [1, 3-5].

An increase in mining depth is systematically associated with an increase in geostatic pressure, leading to elevated stress levels within the rock mass. Concurrently, the influence of horizontal stresses becomes more pronounced, along with their anisotropy, while the structural integrity of the rock mass deteriorates due to progressive fracturing and defect accumulation.

The formation of the in-situ stress field is governed by the interaction of tectonic, gravitational, lithological, and structural factors, resulting in pronounced spatial variability of geomechanical conditions [6–8]. Various techniques have been developed for stress determination, including hydraulic fracturing, acoustic emission monitoring, stress-relief methods, and overcoring [9–12]. Among these, the overcoring method remains one of the most reliable approaches for direct evaluation of stress tensor components in rock masses [9]. Recent improvements in measurement systems and stress inversion techniques have enhanced the accuracy of stress characterization in deep mining environments [10–12]. Nevertheless, direct stress measurements remain costly, spatially limited, and strongly dependent on local geological conditions, highlighting the importance of numerical modeling for stress field reconstruction and geomechanical analysis [11–14].

Under such constraints, numerical modeling becomes an indispensable tool, enabling the integration of experimental observations and geological data to reconstruct a representative stress field. Numerical techniques, including finite element analysis, provide robust capabilities for detailed investigation of stress redistribution, identification of stress concentration zones, and evaluation of rock mass stability [13–15].

Recent numerical investigations have emphasized that the geomechanical response of underground excavations is controlled not only by the magnitude of in-situ stresses but also by the structural characteristics of the rock mass. Imashev et al. [16] demonstrated that stratification significantly influences stress redistribution patterns, deformation localization, and excavation stability. These findings indicate that reliable stability assessment of deep underground openings requires simultaneous consideration of both the stress field and rock mass structural features.

With increasing mining depth, the influence of the in-situ stress state extends beyond purely static deformation processes, giving rise to dynamic geomechanical responses. The most hazardous manifestation of such behavior is rockbursts—sudden brittle failures resulting in violent ejection of rock into excavated spaces and posing a serious threat to underground mining operations.

Both the frequency and intensity of rockbursts exhibit a strong correlation with increasing depth, reflecting elevated in-situ stress levels and the formation of zones of maximum stress concentration around underground excavations. When the stress–strength ratio reaches a critical threshold, the rock mass transitions into an unstable state, leading to dynamic failure.

Contemporary studies identify several principal mechanisms governing rockburst occurrence, primarily categorized into strength-based and energy-based instability mechanisms within the “rock mass–excavation” system. These approaches capture different aspects of rock mass instability and failure development, however, due to the inherently multiscale and nonlinear nature of the phenomenon, a unified theoretical framework has yet to be established.

Recent review studies have provided a comprehensive synthesis of existing approaches to rockburst analysis and prediction. Waqar et al. [17] proposed a classification framework based on occurrence mechanisms, stress sources, failure characteristics, temporal behavior, and loading conditions. The authors also evaluated strength-based, energy-based, deformation-based, and data-driven approaches for assessing rockburst susceptibility, highlighting the need for integrated methodologies capable of accounting for the complex interaction between stress conditions and rock mass behavior.

Recent studies have further emphasized the importance of integrating stress field characterization, numerical modeling, and energy-based approaches for assessing rockburst susceptibility in deep mining environments. Contemporary investigations have demonstrated that stress anisotropy significantly influences failure localization, stress redistribution, and the development of excavation instability. Advances in stress inversion techniques have improved the reconstruction of complex in-situ stress fields in deep underground environments, while modern numerical simulations have provided new insights into the interaction between stress redistribution, plastic zone

evolution and failure development processes. Nevertheless, considerable uncertainty remains regarding the coupled influence of stress conditions, rock mass properties, deformation localization and rock mass failure on the initiation of dynamic instability in deep underground excavations [17–19].

Despite significant advances in the characterization of in-situ stress fields, numerical modeling techniques, and rockburst prediction methods, several important limitations remain. Most previous studies have focused either on stress field characterization, deformation analysis, or rockburst assessment as separate research problems. Furthermore, relatively few investigations have systematically examined the combined influence of stress magnitude, stress anisotropy, and rock mass mechanical properties on deformation behavior, yielded zone evolution within a unified geomechanical framework. Consequently, the quantitative relationships among stress redistribution, deformation localization, yielded zone development, and rockburst potential in deep rock masses remain insufficiently understood. Therefore, the objective of this study is to investigate the influence of in-situ stress conditions on the stress–strain behavior and rockburst potential of deep rock masses through numerical modeling. Particular attention is devoted to the analysis of stress redistribution, deformation localization, and yielded zone development under different stress regimes.

The novelty of this study lies in quantifying the influence of different in-situ stress regimes on the coupled evolution of stress concentration, deformation localization, and yielded zone development around underground excavations. Unlike many previous studies that consider these factors independently, the proposed approach provides an integrated assessment of the mechanisms controlling both excavation stability and rockburst potential in deep rock masses.

The scientific contribution of the study consists in establishing the relationships between in-situ stress conditions, deformation characteristics, yielded zone development, stress concentration, and rockburst susceptibility. It should be emphasized that yielded zones are interpreted as indicators of mechanical instability and stress redistribution rather than direct evidence of dynamic failure. The obtained results provide new insights into the geomechanical response of highly stressed rock masses and contribute to the development of more reliable approaches for stability assessment, excavation design, and geotechnical risk management in deep underground mining environments.

2. Materials and Methods

The objective of this study is to perform a numerical evaluation of the influence of the in-situ stress field on the stress–strain response of the rock mass at considerable depths (600–1500 m). To this end, the finite element method (FEM) was employed using Rocscience RS2, a widely recognized platform for nonlinear geomechanical analysis. Within the adopted problem formulation, the stress distribution was systematically analyzed under varying initial stress conditions, while potential failure zones were delineated using the nonlinear Hoek–Brown strength criterion. The rock mass was represented as an isotropic elasto-plastic medium, with strength parameters assumed to degrade as a function of fracturing intensity and structural heterogeneity. The set of input parameters applied in the numerical simulations is summarized in Table 1.

Table 1. Input parameters for numerical modeling

Parameter	Unit	Value
Uniaxial compressive strength, σ_{ci}	MPa	100
Rock mass deformation modulus, E_m	MPa	8530
Intact-rock modulus	MPa	20000
Unit weight	t/m^3	2.5
mb	–	1.677
s	–	0.0038
a	–	0.50
Geological Strength Index (GSI)	–	50
Poisson's ratio	–	0.26
In-situ stress ratio, k	–	0.8; 1.0; 1.1; 1.2

2.1. Numerical Model Development

The numerical analyses were performed using the finite element software Rocscience RS2 under plane strain conditions. A two-dimensional model representing a deep underground excavation was developed to investigate the influence of in-situ stress conditions on the stress–strain response of the surrounding rock mass.

Figure 1 presents the model adopted for numerical simulations and the excavation parameters used in the analysis. The cross-sectional area of the excavation is 19.82 m². To minimize boundary effects, the dimensions of the numerical domain were selected to be sufficiently larger than the excavation size, ensuring that stress redistribution around the opening was not influenced by artificial boundary constraints.

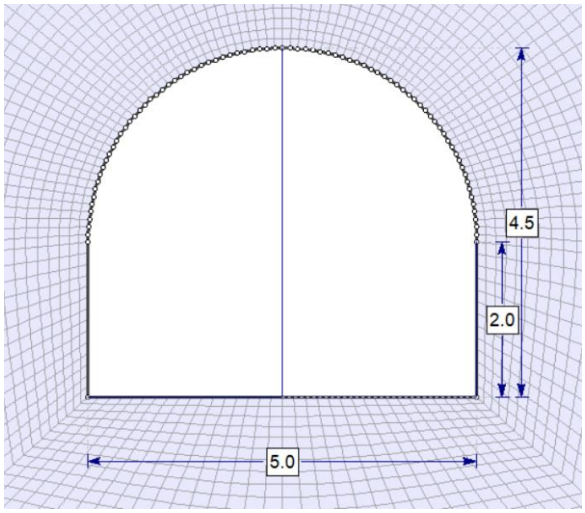

Figure 1. Geometry of the numerical model and excavation dimensions used in the simulations

The rock mass was modeled as an isotropic elasto-plastic medium governed by the nonlinear Hoek–Brown failure criterion. Mechanical properties of the rock mass were derived using the Geological Strength Index (GSI) approach. The rock mass deformation modulus was estimated using the empirical relationship proposed by Hoek & Diederichs [19], while the strength parameters mb, s, and a were determined from the corresponding Hoek–Brown empirical formulations:

$$E_m = E_i\left(0.02 + \frac{1-\frac{D}{2}}{1+e^{\left(\frac{60+15D-GSI}{11}\right)}}\right), MPa \quad (1)$$

where, E_m is the rock mass deformation modulus, *GSI* is the Geological Strength Index, and *D* is the disturbance factor. In this study, $D = 0$ was assumed.

The numerical domain was discretized using an automatically generated finite element mesh. Additional mesh refinement was applied in the vicinity of the excavation boundary to improve the accuracy of stress and deformation calculations in regions characterized by high stress gradients.

2.2. Boundary Conditions and In-Situ Stress Conditions

The initial stress field was assumed to consist of gravitational and tectonic components. The vertical stress was calculated according to:

$$\sigma_v = \gamma H \quad (2)$$

where, γ is the unit weight of the rock mass and H is the depth below the ground surface.

The horizontal stress was determined using the lateral stress coefficient:

$$\sigma_h = k\,\sigma_v \quad (3)$$

where, k represents the ratio between horizontal and vertical stresses.

To evaluate the influence of stress anisotropy, four stress ratios were considered: k = 0.8, 1.0, 1.1, and 1.2. The investigated depth range varied from 600 m to 1500 m, corresponding to conditions commonly encountered in deep underground mining operations.

Normal displacement was restricted along the lateral boundaries of the model, while the bottom boundary was fixed in both horizontal and vertical directions. The upper boundary remained free, allowing the development of excavation-induced deformation.

2.3. Failure Assessment and Rockburst Indicators

The assessment of rock mass stability was conducted based on the Hoek–Brown failure criterion and the analysis of principal stress distributions. Yielded zones were identified as regions where the stress state exceeded the strength envelope of the rock mass.

The values of the rockburst intensity coefficient used for calculating the Turchaninov, Wang, and Castro rockburst criteria were obtained directly from the stress distributions generated in the RS2 software according to the criteria presented in Table 2. For each simulation case, the values corresponding to the largest zone distributed along the excavation boundary and delineated by contour lines were selected. The maximum coefficient values obtained in this

manner were subsequently used to calculate the rockburst susceptibility indices. The use of maximum contour-derived values was considered justified because rockburst initiation is generally associated with localized zones of stress concentration rather than with average stress conditions within the rock mass.

Particular attention was paid to the development of plastic zones surrounding the excavation, as their formation is directly related to stress concentration and excavation instability. The obtained results were subsequently analyzed in terms of stress redistribution, deformation localization, yielded zone propagation, and potential dynamic instability under varying depth and principal stress ratio conditions. The adopted numerical modeling approach is based on the widely accepted Hoek–Brown failure criterion and finite element formulation implemented in RS2. The obtained stress redistribution patterns and yielded zone development are consistent with observations reported in previous studies of deep underground excavations [7, 16, 18-22], providing confidence in the reliability of the modeling results.

The overall workflow adopted for the numerical investigation is presented in Figure 2.

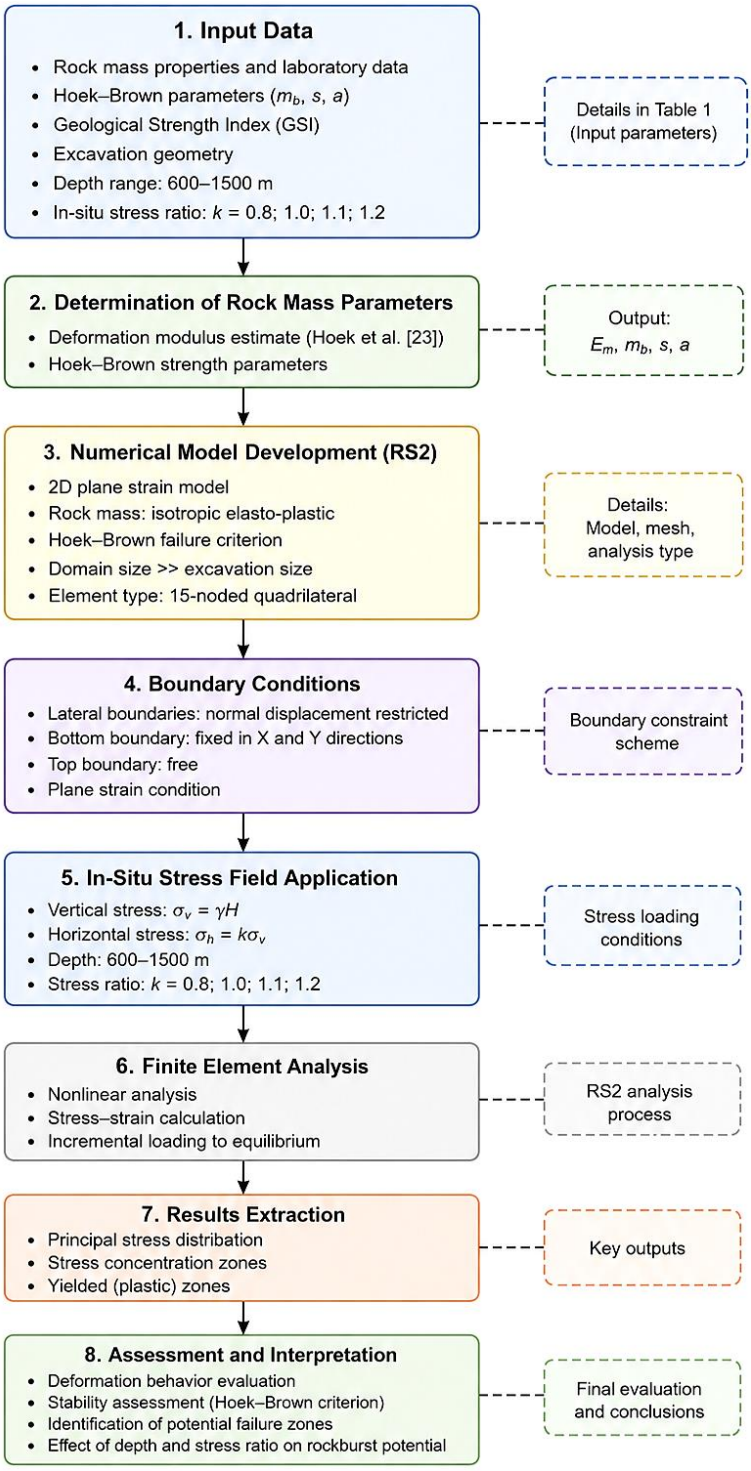

Figure 2. Methodological workflow of the numerical investigation

3. Results and Discussion

3.1. Assessment of the Stress State of the Rock Mass at Great Depths

To assess the stress condition of the rock mass at great depths, as well as the influence of depth on stress distribution, a depth range from 600 m to 1500 m was considered under a hydrostatic in-situ stress field. Figure 3 presents the results of numerical modeling, including the distribution of stresses and the formation of plastic zone around the excavation within the rock mass.

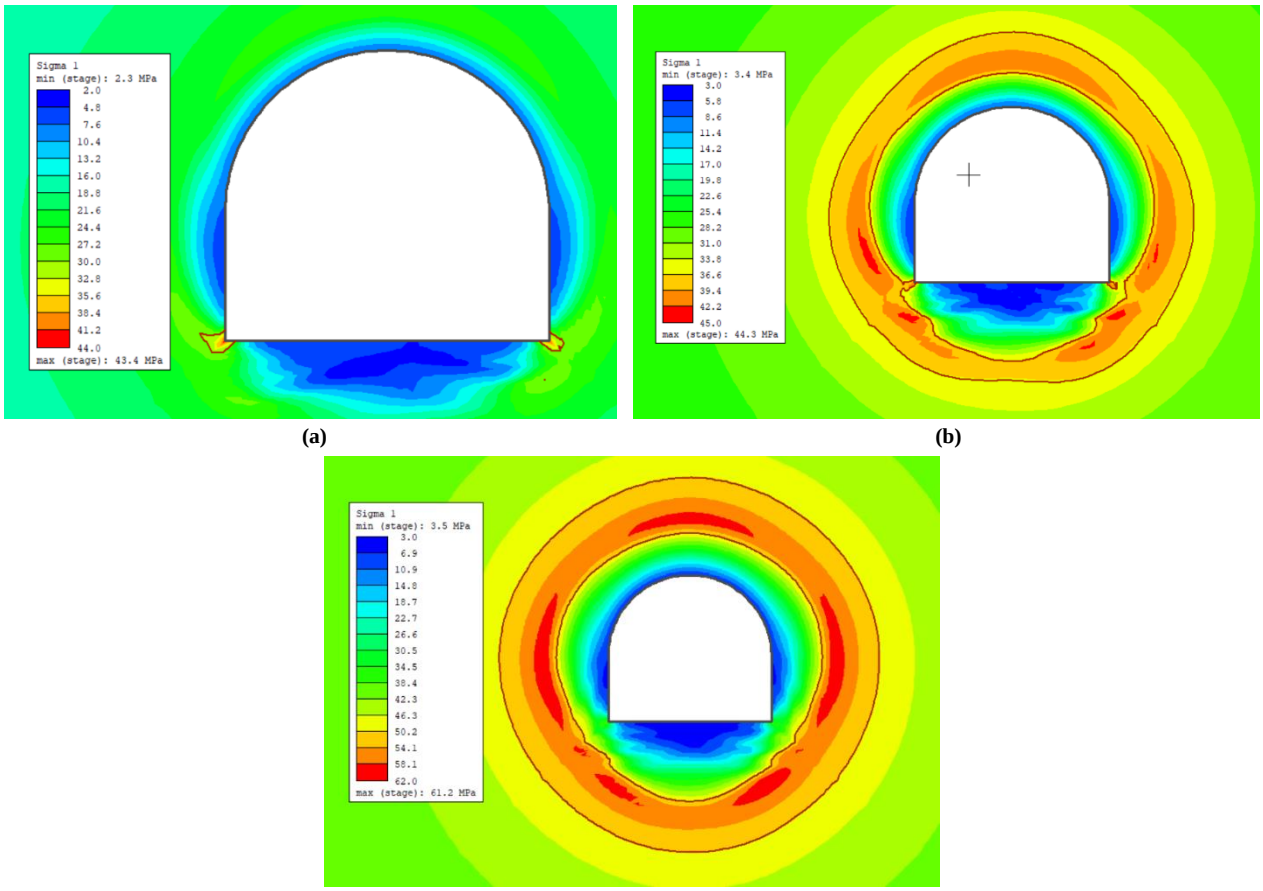

(a) **(b)**

(c)

Figure 3. Formation of principal stresses in the rock mass around the excavation at different depths: (a) 600 m; (b) 1000 m; (c) 1500 m

The numerical modeling results presented in Figure 3 demonstrate the spatial distribution of the maximum principal stress (P_{max}) in the vicinity of the excavation. An increase in depth is accompanied by a systematic increase in stress magnitude, as well as by a pronounced intensification of stress concentration near the excavation boundary. At a depth of 600 m, stress concentrations are predominantly localized at the junctions of the sidewalls and the floor, exhibiting relatively moderate intensity. At 1000 m, a well-defined high-stress zone develops along the entire excavation contour, characterized by sharper stress gradients. At 1500 m, P_{max} exhibits significant concentration around the excavation, particularly within the roof and lateral zones, while regions of stress relief become increasingly localized. In general, increasing depth results not only in elevated stress levels but also in a substantial redistribution of stresses, leading to the formation of stable stress concentration zones and a more complex stress–strain state of the rock mass.

The obtained results are consistent with the well-established understanding that increasing mining depth leads to a proportional increase in geostatic stress and excavation-induced stress concentration. Similar observations have been reported by Martin & Chandler [15], who demonstrated that highly stressed hard rock masses exhibit progressive stress redistribution and localized failure around underground openings. A comparable tendency was also reported by Brady & Brown [4], who emphasized that stress concentration around excavations becomes increasingly pronounced with depth, resulting in reduced rock mass stability.

The numerical simulations further indicate that stress concentration is predominantly localized in the roof and sidewall regions of the excavation. This behavior can be explained by the redistribution of the principal stresses around the excavation contour and the formation of compressive stress arches. As depth increases, the magnitude of the maximum principal stress grows substantially, resulting in larger stress gradients and more extensive yielded zones. Such conditions are widely recognized as precursors to excavation instability and dynamic failure in deep underground environments.

3.1.1. Rockburst Prediction Methods

Rockburst prediction remains an important challenge in rock mechanics and deep underground mining. Numerous approaches have been developed to assess rockburst susceptibility, including empirical, analytical, numerical, laboratory-based, and monitoring-based methods. Among these approaches, strength-based and energy-based criteria are the most widely applied in engineering practice.

Strength-based criteria evaluate the relationship between the induced stress state and the strength characteristics of the rock mass, whereas energy-based approaches focus on the accumulation and release of elastic strain energy as a mechanism of dynamic failure. Although considerable progress has been achieved in understanding rockburst mechanisms, no universally accepted criterion currently exists, and different prediction methods may provide different hazard assessments for the same geological conditions.

According to the review by Waqar et al. [17], numerous rockburst prediction criteria have been proposed within the framework of strength-based and energy-based concepts. In the present study, emphasis is placed on strength-based approaches because they can be directly applied to the stress distributions obtained from numerical modeling.

The Turchaninov, Wang, and Castro criteria were selected because they represent widely applied strength-based approaches and provide complementary perspectives for the preliminary assessment of rockburst susceptibility in underground excavations. The criteria adopted in this study are summarized in Table 2. Rockburst intensity was subsequently evaluated using the numerical modeling results obtained for different mining depths and stress conditions.

Table 2. Rockburst strength criteria

Researchers	Formula	Rockburst intensity				
		None	Light	Medium	Heavy	Serious
Turchaninov et al. [23]	$(\sigma_1 + \sigma_2)/\sigma_{ci}$	≤0.3	0.3-0.5	0.5-0.8	≥0.8	-
Castro et al. [24]	$(\sigma_1 - \sigma_3)/\sigma_{ci}$	<0.45	0.45-0.6	0.6-0.7	>0.7	-
Wang & Cai [25]	$\sigma_\theta^{max}/\sigma_{ci}$	-	0.3-0.5	0.5-0.7	0.7-0.9	>0.9

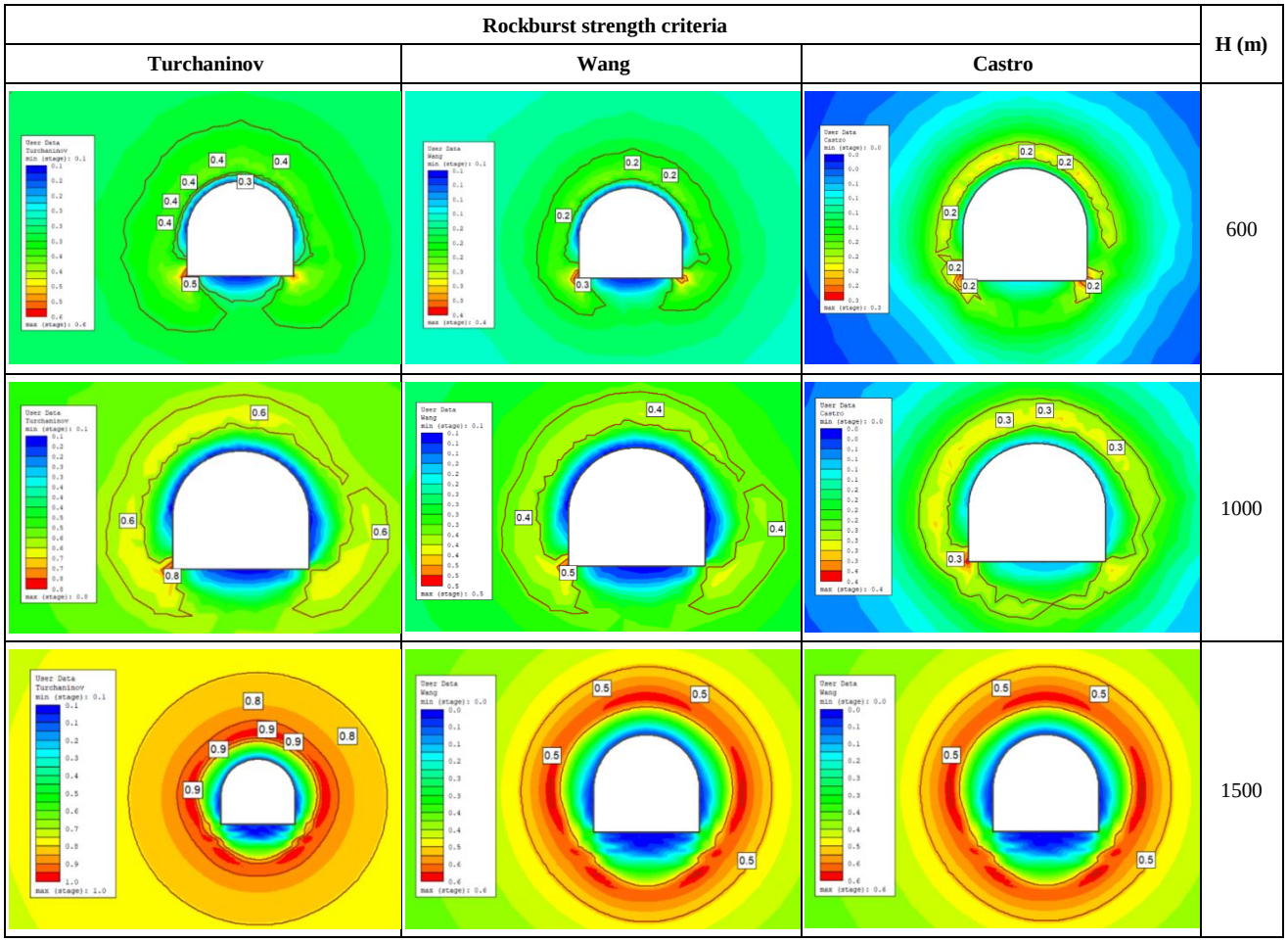

Figure 4. Numerical modeling of hazardous zones around the excavation based on rockburst potential criteria at different depths

Figure 4 presents a comparison of stress distribution and damage zones around an arched excavation at depths of 600, 1000, and 1500 m according to the Turchaninov, Wang, and Castro strength criteria. The modeling results demonstrate that increasing mining depth leads to a systematic increase in stress concentration and expansion of the failure zone around the excavation contour, indicating an increased rockburst hazard of the surrounding rock mass.

At a depth of 600 m, all criteria indicate a relatively stable rock mass condition with localized stress concentration zones mainly occurring in the roof and at the junctions between the arch and the sidewalls. With increasing depth to 1000 m, a pronounced ring-shaped stress redistribution zone develops, while the maximum stress concentrations are observed in the roof and sidewall regions of the excavation. At a depth of 1500 m, the formation of a continuous damage zone around the excavation is observed, indicating the transition of the rock mass into a highly rockburst-prone state.

The comparative analysis showed that the Turchaninov criterion predicts the highest stress concentration values and is the most sensitive to brittle rock failure. In contrast, the Wang and Castro criteria exhibit smoother stress distributions and better reflect the development of plastic deformation within the near-contour rock mass. Overall, the results confirm that increasing mining depth significantly elevates the risk of dynamic ground pressure manifestations and necessitates the implementation of reinforced support systems and comprehensive geomechanical monitoring.

A comparison of the three rockburst criteria reveals noticeable differences in the predicted extent of hazardous zones. The Turchaninov criterion consistently identifies larger regions of elevated rockburst susceptibility compared with the Wang and Castro criteria. This difference is primarily associated with the mathematical formulation of the criterion, which is based on the relationship between principal stresses and uniaxial compressive strength and therefore exhibits greater sensitivity to stress concentration effects.

In contrast, the Wang and Castro criteria provide more conservative predictions and are less sensitive to local stress peaks. Similar discrepancies among strength-based rockburst criteria have been reported in recent review studies [16–19], which concluded that different prediction methods often produce substantially different hazard classifications for the same geological conditions. This observation highlights the importance of applying multiple criteria simultaneously when evaluating rockburst susceptibility in deep underground excavations.

The agreement among all three criteria regarding the increasing rockburst hazard with depth provides additional confidence in the reliability of the numerical results. Although the absolute hazard levels differ, the overall trend remains consistent, indicating that depth is one of the dominant factors controlling rockburst potential.

As shown in Figure 5, the evolution of rockburst intensity, assessed using various methodological approaches (Turchaninov, Wang, and Castro) based on rock mass strength criteria, demonstrates a consistent increasing trend with depth. This trend reflects the progressive deterioration of geomechanical conditions and, consequently, the increasing susceptibility of the rock mass to dynamic failure under elevated in-situ stress levels.

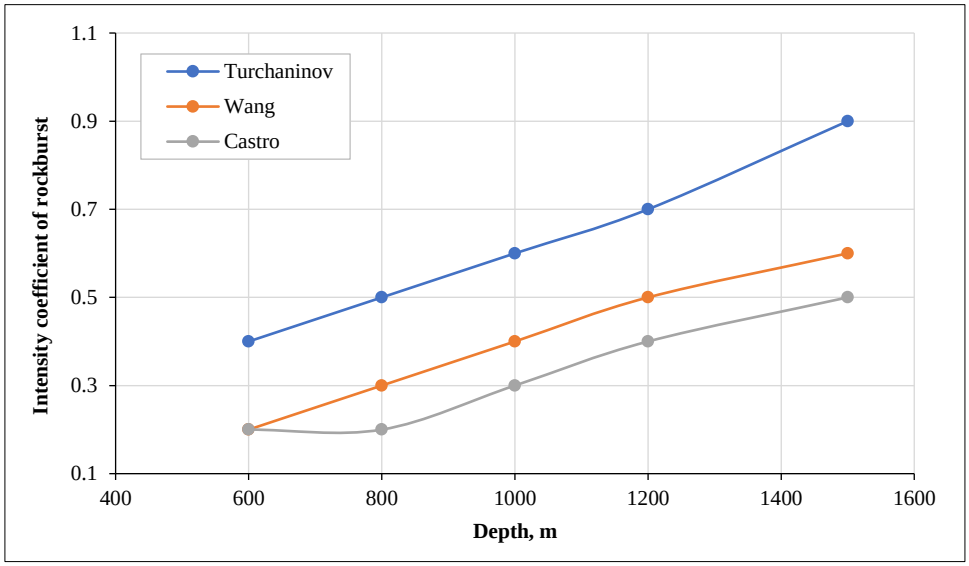

Figure 5. Dependence of the rockburst hazard coefficient on mining depth

Figure 5 illustrates the relationship between the rockburst intensity coefficient and mining depth according to the criteria proposed by Turchaninov, Wang, and Castro. The graph analysis was carried out based on the classification presented in Table 2.

As the mining depth increases, the rockburst intensity coefficient also increases for all considered methods, indicating a higher tendency of the rock mass toward dynamic manifestations of rock pressure. However, the pattern of change and the estimated intensity levels differ among the researchers.

According to the Turchaninov criterion, the coefficient values increase from 0.4 at a depth of 600 m to 0.9 at 1500 m. Based on Table 2, at depths of 600–800 m the rock mass corresponds to a low-intensity category (0.3–0.5), while in the range of 1000–1200 m it reaches a medium intensity level (0.5–0.8). At a depth of 1500 m, the condition corresponds to a heavy rockburst category (≥0.8). This criterion demonstrates the highest sensitivity to increasing depth.

According to the Wang criterion, the coefficient varies from 0.2 to 0.6. At a depth of 600 m, the hazard level is absent or minimal, while at depths of 800–1000 m a low-intensity rockburst condition is observed (0.3–0.5). Beginning from 1200 m, the condition transitions to medium intensity (0.5–0.7). The values do not reach the heavy or very heavy rockburst categories.

According to the Castro criterion, the coefficient increases from 0.2 to 0.5. In the depth interval of 600–800 m, the rock mass condition corresponds to no or low rockburst probability (<0.45), whereas at depths of 1000–1500 m the massif is classified as prone to weak dynamic manifestations (0.45–0.6). The Castro criterion provides the most conservative assessment of rockburst intensity. Thus, all methods confirm that the risk of rockburst increases with mining depth. However, the Turchaninov criterion predicts a significantly higher intensity level compared to the Wang and Castro criteria.

The depth-dependent increase in rockburst susceptibility obtained in this study is consistent with findings reported in numerous investigations of deep mining environments. Li et al. [18] demonstrated that elevated in-situ stress levels significantly increase the probability of dynamic failure and emphasized the importance of stress-based and energy-based indicators for rockburst prediction. Similarly, Hoek & Diederichs [19] showed that rockburst intensity tends to increase rapidly once critical stress thresholds are exceeded, particularly under conditions of high stress anisotropy.

Recent studies employing numerical modeling techniques have also reported that increasing depth promotes the development of extensive stress concentration zones and larger plastic regions surrounding underground excavations [18–20]. The present results support these observations and further demonstrate that stress concentration, yielded zone evolution, and rockburst potential exhibit a strong coupled relationship.

From an engineering perspective, the obtained results indicate that underground excavations located at depths exceeding approximately 1000 m require enhanced geomechanical monitoring and support design measures. The progressive increase in stress concentration and rockburst susceptibility observed in the simulations suggests that conventional support systems may become insufficient under deep mining conditions, necessitating the application of dynamic support technologies and continuous stress monitoring systems.

3.2. Assessment of the Influence of the In-Situ Stress Field on the Formation of Plastic Zones as a Function of Mining Depth

The development of plastic deformation zones around underground excavations is governed by stress redistribution processes induced by rock mass unloading during mining operations. Numerous studies have shown that a plastic zone forms in the vicinity of the excavation boundary, with its size and geometry controlled by the initial stress state, excavation configuration, and the mechanical properties of the rock mass [18]. Under conditions of increasing depth and elevated in-situ stresses, the internal structure of these zones becomes more complex, incorporating regions of hardening, softening, and residual deformation, thereby reflecting the intrinsically nonlinear behavior of rock materials. Furthermore, tectonic disturbances and structural heterogeneity contribute to stress field asymmetry and promote the expansion of yielded zones, leading to a reduction in excavation stability [16].

In practical settings, underground excavations are typically subjected to complex, non-hydrostatic stress conditions. Consequently, the investigation of plastic zone evolution under varying lateral stress coefficients is of critical importance for excavation design and the maintenance of mining safety. The lateral stress coefficient is defined as $k = P_h/P_v$, where P_h is assumed to be equal to P_z, and the maximum principal stress varies within the range of 25–42.5 MPa.

As illustrated in Figure 6, the spatial distribution of yielded zones around the excavation is strongly dependent on the value of the lateral stress coefficient. At $k = 0.8$, the yielded zone is predominantly concentrated in the lower part of the excavation, where the stress levels are highest, while the roof and sidewalls experience comparatively lower plastic zone area. At $k = 1.1$, the yielded zone becomes more evenly distributed; however, the floor remains the most highly stressed region, and the contribution of sidewall plastic deformation area increases. At $k = 1.2$, the yielded zone pattern approaches a near-uniform distribution along the excavation contour, with more pronounced deformation observed in the sidewalls.

With increasing depth, the overall intensity of plastic deformation increases, accompanied by a progressive expansion of the plastic zone due to the growth of the initial stress field. Simultaneously, an increase in the lateral stress coefficient leads to a redistribution of loading from the floor toward the sidewalls. At greater depths, these

effects are further amplified, resulting in both the intensification and spatial enlargement of yielded zones surrounding the excavation.

This behavior can be explained by the progressive increase in horizontal compressive stresses. As the stress ratio k increases, a larger proportion of the load is transferred to the sidewalls, leading to the activation of shear-dominated failure mechanisms. Consequently, the localization of yielded zones gradually shifts from the excavation floor toward the lateral boundaries. Similar trends have been reported in numerical and experimental studies of deep underground openings subjected to anisotropic stress fields [18, 20].

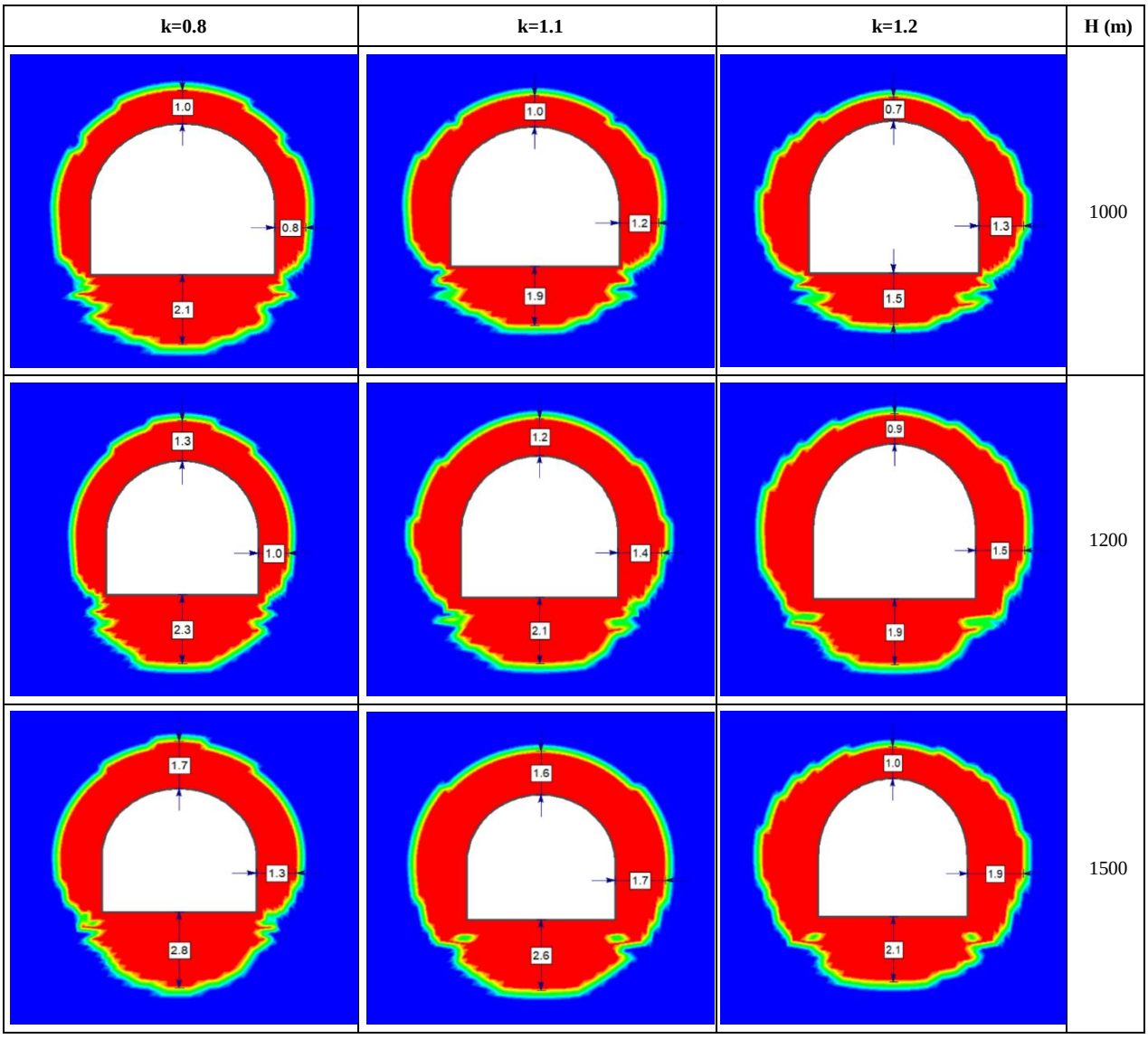

Figure 6. Development of the plastic zone around the excavation under different initial stress field conditions as a function of mining depth

Figure 6 presents the spatial distribution of yielded zones around the excavation for different values of the lateral stress coefficient (k = 0.8, 1.1, 1.2) at depths of 1000, 1200, and 1500 m. An increase in depth is associated with a systematic expansion of the plastic zone and an increase in deformation intensity, which is directly related to the growth of geostatic stresses.

At a low value of k = 0.8, the yielded zone is predominantly localized in the lower part of the excavation. As the lateral stress coefficient increases (k = 1.1–1.2), the yielded zone is progressively redistributed toward the sidewalls, resulting in a more uniform distribution along the excavation contour. The most extensive development of the plastic zone is observed at a depth of 1500 m, where the rock mass experiences the highest stress levels.

In general, increasing depth leads to the intensification of yield zone processes, while higher values of the lateral stress coefficient primarily control their spatial distribution around the excavation. Figures 7–9 provide a more detailed characterization of the governing patterns of plastic zone evolution as a function of depth and the initial stress field.

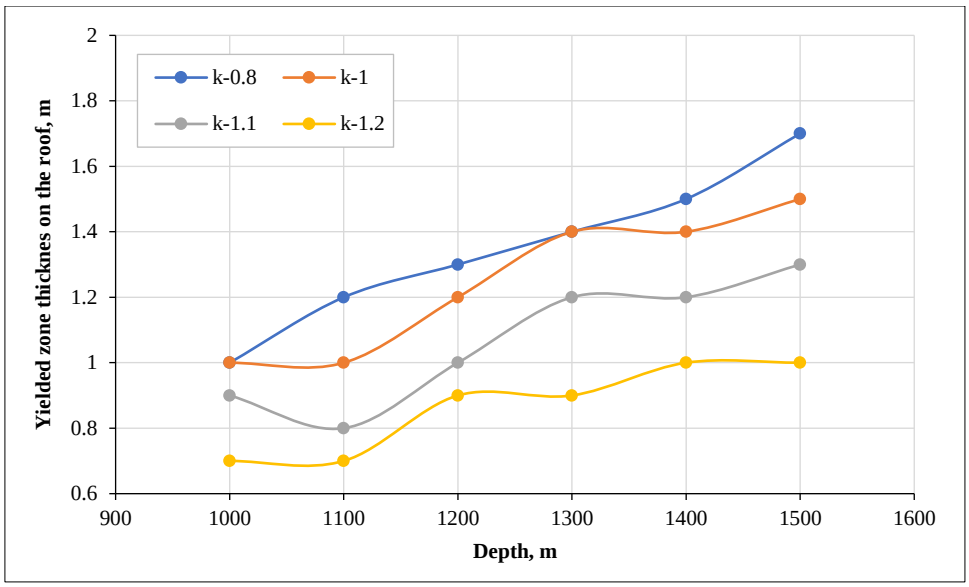

Figure 7. Distribution of the yielded zone thickness along the excavation roof as a function of depth

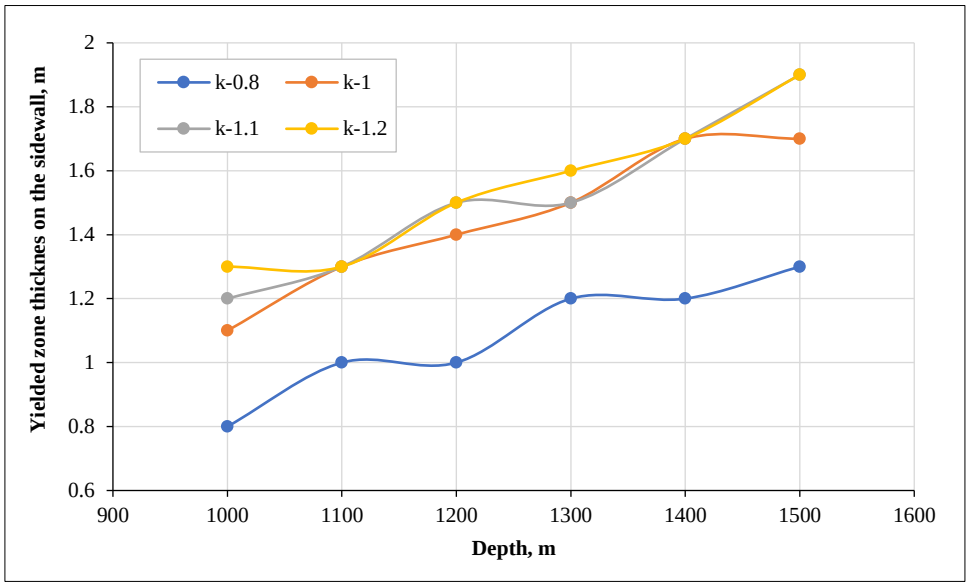

Figure 8. Distribution of the yielded zone thickness along the sidewalls as a function of excavation depth

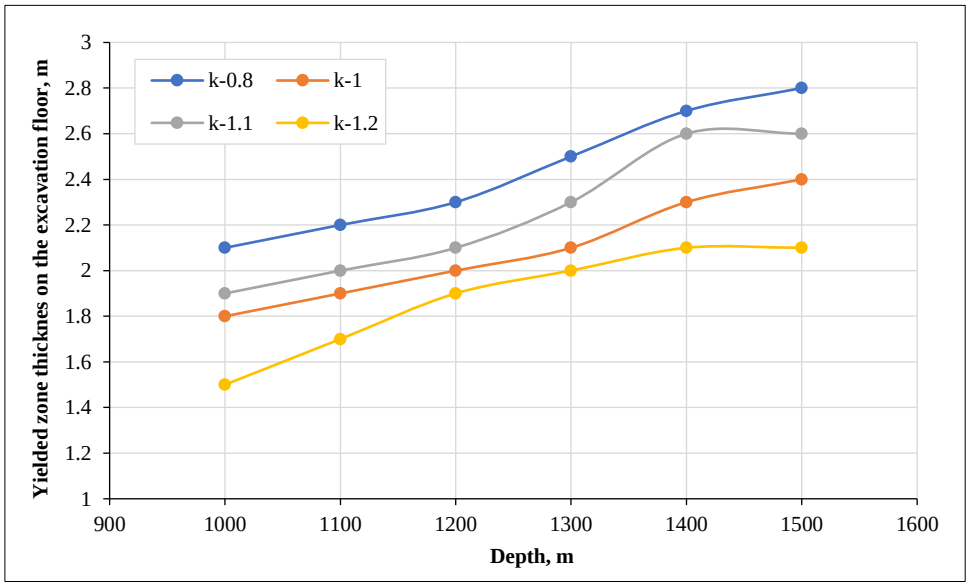

Figure 9. Distribution of the yielded zone thickness along the excavation floor as a function of depth

A generalized analysis of the relationships describing the distribution of yielded zones in the roof, sidewalls, and floor of the excavation (Figures 7–9) allows for the identification of consistent patterns governing the influence of depth and the lateral stress coefficient (k) on the stress–strain state of the rock mass.

Across the entire investigated depth range (1000–1500 m), a systematic expansion of yielded zones is observed in all elements of the excavation contour. This trend is directly associated with the increase in geostatic stresses and the resulting expansion of stress concentration and yielded zones within the rock mass. At the same time, the spatial distribution of deformation is strongly controlled by the ratio of horizontal to vertical stresses, as defined by the coefficient k.

The analysis of roof behavior indicates that, at lower values of k (k = 0.8), more extensive yielded zones develop due to the dominant influence of vertical stress. As k increases, stress redistribution occurs, resulting in a reduction of deformation concentration in the roof and a partial transfer of loading to the sidewalls. This behavior reflects a decreasing contribution of bending–tensile failure mechanisms in the roof with increasing horizontal stress levels.

In contrast, the sidewalls exhibit an opposite trend: an increase in k leads to a significant expansion of yielded zones. At k = 1.2, the sidewalls become the most highly stressed components of the system, indicating the predominance of shear failure mechanisms under elevated horizontal compression. With increasing depth, this effect becomes more pronounced, and the sidewalls assume a controlling role in the development of the overall instability zone.

The observed influence of stress anisotropy on yielded zone localization is consistent with previous studies emphasizing the role of rock mass structure and geological discontinuities in controlling excavation stability. Imashev et al. [16] reported that variations in rock mass structure significantly affect stress redistribution and deformation patterns around underground openings. The present results further indicate that, even in an equivalent rock mass representation, the ratio of principal stresses remains a dominant factor governing the spatial development of yielded zones and potential instability regions.

The excavation floor consistently exhibits the highest levels of plastic deformation across all considered conditions, which is attributed to the concentration of vertical stresses and the confining effect of the surrounding rock mass. At lower values of k (i.e. k = 0.8), yielded zone in the floor reaches its maximum, whereas an increase in k leads to a partial reduction in deformation intensity due to stress redistribution toward the sidewalls. Nevertheless, even at higher values of k, the floor remains one of the most critical elements in terms of structural stability.

Overall, the integrated analysis of the three graphs demonstrates that increasing depth results in both the expansion of yielded zones and a greater complexity of the stress–strain state of the rock mass, while the lateral stress coefficient governs the spatial localization of these deformations. At low k values, deformation is predominantly concentrated in the roof and floor, corresponding to tensile and bending-dominated failure mechanisms. In contrast, higher k values promote a transition toward a more uniform deformation distribution dominated by shear mechanisms, with the sidewalls playing a leading role. These findings are consistent with established theoretical concepts of stress redistribution in rock masses and highlight the importance of accounting for the principal stress ratio in the assessment of excavation stability at great depths.

It should be noted that the presence of yielded zones does not automatically indicate the occurrence of a rockburst. Plastic deformation may act as a stress-relief mechanism and contribute to the redistribution of stresses around the excavation. However, under deep mining conditions characterized by high stress levels and brittle rock behavior, the development of localized yielded zones may coexist with the accumulation of substantial elastic strain energy in adjacent rock volumes. In such cases, failure localization can serve as a precursor to dynamic instability rather than a direct indicator of rockburst occurrence. Therefore, in the present study, yielded zones are interpreted as indicators of potential instability and stress concentration, while rockburst susceptibility is assessed separately using established rockburst criteria.

The obtained results are in good agreement with previous investigations of deep underground excavations. Recent numerical and experimental studies have demonstrated that increasing stress anisotropy significantly affects the geometry of yielded zones, promotes deformation localization, and influences excavation stability. The trends observed in the present study further support these findings and indicate that the ratio of principal stresses is a governing parameter controlling deformation localization in deep rock masses. Furthermore, the progressive expansion of yielded zones with depth observed in this study confirms the strong relationship between stress concentration, plastic deformation, and excavation instability under deep mining conditions [16, 18].

4. Conclusion

This study investigated the influence of in-situ stress conditions on the stress–strain behavior, yielded zone development, and rockburst potential of deep rock masses through numerical modeling using the finite element method and the Hoek–Brown failure criterion. The analyses were performed for mining depths ranging from 600 to 1500 m and for different lateral stress coefficients (k = 0.8–1.2), enabling a comprehensive assessment of the role of stress magnitude and stress anisotropy in controlling excavation stability.

The results demonstrate that increasing mining depth leads to a substantial increase in stress concentration around underground excavations and promotes the progressive expansion of yielded zones. At depths exceeding 1000 m, stress redistribution becomes significantly more pronounced, resulting in the formation of extensive high-stress regions around the excavation contour. The numerical simulations revealed that the geometry and localization of yielded zones are strongly dependent on the ratio between horizontal and vertical stresses. At relatively low values of the lateral stress coefficient, deformation is concentrated primarily in the roof and floor, whereas higher stress ratios promote the redistribution of loading toward the sidewalls and increase the contribution of shear-dominated failure mechanisms.

The analysis of rockburst susceptibility using the Turchaninov, Wang, and Castro criteria confirmed that the potential for dynamic failure systematically increases with depth. Although the criteria predict different hazard levels, all methods indicate a consistent trend of increasing rockburst susceptibility under elevated stress conditions. The Turchaninov criterion was found to be the most sensitive to stress concentration effects, while the Wang and Castro criteria provided more conservative assessments.

The obtained results highlight the coupled influence of stress magnitude and stress anisotropy on the geomechanical response of deep rock masses. The study demonstrates that excavation stability cannot be reliably assessed on the basis of mining depth alone, since the ratio of principal stresses exerts a comparable influence on deformation localization and failure development. From an engineering perspective, the findings emphasize the necessity of incorporating realistic in-situ stress conditions into numerical analyses and support design procedures for deep underground excavations. The proposed approach contributes to a better understanding of excavation instability mechanisms and provides a basis for improving geomechanical risk assessment and rockburst hazard management in deep mining environments.

5. Declarations

5.1. Author Contributions

Conceptualization, A.I. and G.Y.; methodology, A.S.; software, G.Y. and G.Z.; formal analysis, A.I.; investigation, M.G.; resources, A.I. and M.G.; data curation, G.Y.; writing—original draft preparation, G.Y.; writing—review and editing, A.I.; visualization, A.S.; supervision, A.I.; project administration, G.Y. All authors have read and agreed to the published version of the manuscript.

5.2. Data Availability Statement

The data presented in this study are available on request from the corresponding author.

5.3. Funding

This research has been funded by the Science Committee of the Ministry of Science and Higher Education of the Republic of Kazakhstan (Grant No. AP22787307).

5.4. Institutional Review Board Statement

Not applicable.

5.5. Informed Consent Statement

Not applicable.

5.6. Declaration of Competing Interest

The authors declare that there are no conflicts of interest concerning the publication of this manuscript. Furthermore, all ethical considerations, including plagiarism, informed consent, misconduct, data fabrication and/or falsification, double publication and/or submission, and redundancies have been completely observed by the authors.

6. References

[1] Amadei, B., & Stephansson, O. (1997). Rock Stress and Its Measurement. Springer, Dordrecht, Germany. doi:10.1007/978-94-011-5346-1.

[2] Zang, A., & Stephansson, O. (2010). Stress field of the earth's crust. Springer, Dordrecht, Germany. doi:10.1007/978-1-4020-8444-7.

[3] Hudson, J., Harrison, J., & Popescu, M. (2002). Engineering Rock Mechanics: An Introduction to the Principles. Applied Mechanics Reviews, 55(2), 1451165. Pergamon Press. doi:10.1115/1.1451165.

[4] Brady, B. H. G., & Brown, E. T. (1993). Rock mechanics for underground mining. Springer, Dordrecht, Germany. doi:10.1007/978-1-4020-2116-9.

[5] Hoek, E., & Brown, E. T. (1980). Empirical strength criterion for rock masses. Journal of the Geotechnical Engineering Division, ASCE, 106(GT9, Proc. Paper, 15715), 1013–1035. doi:10.1061/ajgeb6.0001029.

[6] Brown, E. T., & Hoek, E. (1978). Trends in relationships between measured in-situ stresses and depth. International Journal of Rock Mechanics and Mining Sciences & Geomechanics Abstracts, 15(4), 211–215. doi:10.1016/0148-9062(78)91227-5.

[7] Stephansson, O., & Zang, A. (2012). ISRM Suggested Methods for Rock Stress Estimation—Part 5: Establishing a Model for the in Situ Stress at a Given Site. Rock Mechanics and Rock Engineering, 45(6), 955–969. doi:10.1007/s00603-012-0270-x.

[8] Hast, N. (1958). The measurement of rock pressure in Mines. Sveriges Geologiska Undersokning, Arsbok, 45(58), 152–170.

[9] Haimson, B. C., & Cornet, F. H. (2003). ISRM suggested methods for rock stress estimation-part 3: Hydraulic fracturing (HF) and/or hydraulic testing of pre-existing fractures (HTPF). International Journal of Rock Mechanics and Mining Sciences, 40(7–8), 1011–1020. doi:10.1016/j.ijrmms.2003.08.002.

[10] Zoback, M. D. (2007). Reservoir Geomechanics. Cambridge University Press, Cambridge, United Knigdom. doi:10.1017/CBO9780511586477.

[11] Herget, G. (1993). Rock Stresses and Rock Stress Monitoring in Canada. Rock Testing and Site Characterization, 473–496. doi:10.1016/b978-0-08-042066-0.50026-4.

[12] Jing, L., & Hudson, J. A. (2002). Numerical methods in rock mechanics. International Journal of Rock Mechanics and Mining Sciences, 39(4), 409–427. doi:10.1016/S1365-1609(02)00065-5.

[13] Jing, L. (2003). A review of techniques, advances and outstanding issues in numerical modelling for rock mechanics and rock engineering. International Journal of Rock Mechanics and Mining Sciences, 40(3), 283–353. doi:10.1016/S1365-1609(03)00013-3.

[14] Gurevich, A. E., & Chilingarian, G. V. (1993). Petroleum related rock mechanics. Journal of Petroleum Science and Engineering, 9(4), 352. doi:10.1016/0920-4105(93)90066-n.

[15] Martin, C. D., & Chandler, N. A. (1994). The progressive fracture of Lac du Bonnet granite. International Journal of Rock Mechanics and Mining Sciences & Geomechanics Abstracts, 31(6), 643–659. doi:10.1016/0148-9062(94)90005-1.

[16] Imashev, A., Suimbayeva, A., Zhunusbekova, G., Adoko, A. C., & Issakov, B. (2024). Assessing stability of mine workings driven in stratified rock mass. Mining of Mineral Deposits, 18(1), 82–88. doi:10.33271/mining18.01.082.

[17] Waqar, M. F., Guo, S., & Qi, S. (2023). A Comprehensive Review of Mechanisms, Predictive Techniques, and Control Strategies of Rockburst. Applied Sciences (Switzerland), 13(6), 3950. doi:10.3390/app13063950.

[18] Li, H., Yang, Y., Zhang, Z., & Tang, L. (2025). Prediction and classification technology of rockburst hazard in deep buried and high in-situ stress tunnel. Scientific Reports, 15(1), 9633. doi:10.1038/s41598-025-93351-4.

[19] Hoek, E., & Diederichs, M. S. (2006). Empirical estimation of rock mass modulus. International Journal of Rock Mechanics and Mining Sciences, 43(2), 203–215. doi:10.1016/j.ijrmms.2005.06.005.

[20] Imashev, A., Mussin, A., & Adoko, A. C. (2024). Investigating an Enhanced Contour Blasting Technique Considering Rock Mass Structural Properties. Applied Sciences (Switzerland), 14(23), 11461. doi:10.3390/app142311461.

[21] Mussin, A., Imashev, A., Yeskenova, G., Matayev, A., Suimbayeva, A., Zhunusbekova, G., & Shaike, N. (2025). Numerical Assessment of Inter-Pillar Stability in Inclined Ore Bodies for Underground Mining Design. Civil Engineering Journal, 11(9), 3653–3673. doi:10.28991/CEJ-2025-011-09-06.

[22] Ananin, A., Tungushbayeva, Z., Nurshaiykova, G., Akylbaeva, A., Imashev, A., Zeitinova, S., & Gabitova, A. (2025). Using Geoinformation Technologies for Evaluation and Resilience Forecast of Open Pit Walls. Journal of Human, Earth, and Future, 6(3), 571–584. doi:10.28991/HEF-2025-06-03-06.

[23] Turchaninov, I. A., Markov, G. A., Gzovsky, M. V., Kazikayev, D. M., Frenze, U. K., Batugin, S. A., & Chabdarova, U. I. (1972). State of stress in the upper part of the Earth's crust based on direct measurements in mines and on tectonophysical and seismological studies. Physics of the Earth and Planetary Interiors, 6(4), 229–234. doi:10.1016/0031-9201(72)90005-2.

[24] Castro, L. A. M., Bewick, R. P., & Carter, T. G. (2012). An overview of numerical modelling applied to deep mining. Innovative Numerical Modelling in Geomechanics, 393–414. doi:10.1201/b12130-22.

[25] Wang, X. & Cai, M. (2017). Coupled Numerical Analysis of Ground Motion near Excavation Boundaries in Underground Mines. Rock and Soil Mechanics, 38, 3347–3354.